The Astrophysical Journal Letters, 859:L25 (4pp), 2018 June 1 https://doi.org/10.3847/2041-8213/aac649

The Growth of Stellar Mass Black Hole Binaries Trapped in the Accretion Disks of Active Galactic Nuclei

Shu-Xu Yi[1], K. S. Cheng[1], and Ronald E. Taam[2,3]
[1] Department of Physics, The University of Hong Kong, Hong Kong; yishuxu@hku.hk
[2] Academia Sinica Institute of Astronomy and Astrophysics, Taipei 10617, Taiwan; hrspksc@hku.hk
[3] Department of Physics & Astronomy, Northwestern University, 2145 Sheridan Road, Evanston, IL 60208, USA; taam@asiaa.sinica.edu.tw
Received 2018 March 19; revised 2018 May 16; accepted 2018 May 17; published 2018 June 1

Abstract

Among the four black hole (BH) binary merger events detected by the Laser Interferometer Gravitational-Wave Observatory (LIGO), six progenitor BHs have masses greater than $20\,M_{\odot}$. The existence of such massive BHs suggests that extreme metal-poor stars are the progenitors. An alternative possibility, that a pair of stellar mass BHs each with mass $\sim 7\,M_{\odot}$ increases to $>20\,M_{\odot}$ via accretion from a disk surrounding a supermassive BH (SMBH) in an active galactic nucleus (AGN), is considered. The growth of mass of the binary and the transfer of orbital angular momentum to the disk accelerates the merger. Based on the recent numerical work of Tang et al., it is found that, in the disk of a low-mass AGN with mass $\sim 10^6\,M_{\odot}$ and Eddington ratio >0.01, the mass of an individual BH in the binary can grow to $>20\,M_{\odot}$ before coalescence, provided that accretion takes place at a rate more than 10 times the Eddington value. This mechanism predicts a new class of gravitational wave (GW) sources involving the merger of two extreme Kerr black holes associated with AGNs and a possible electromagnetic wave counterpart.

Key words: galaxies: nuclei – gravitational waves – stars: black holes

1. Introduction

Since the first detection of gravitational waves (GWs) by the Laser Interferometer Gravitational-Wave Observatory (LIGO) in 2015, there have been four confirmed binary black hole (BH) merger events (Abbott et al. 2016a, 2016b, 2017a, 2017b). Six out of the total eight progenitor BHs have mass $\gtrsim 20\,M_{\odot}$, which may point to new formation mechanisms other than the traditional stellar evolutionary channels. Specifically, Fryer & Kalogera (2001) theoretically estimated the mass distribution of BHs as the evolutionary remnant of massive stars (except for population III stars). The mass of BHs formed in this way cannot be in excess of $\sim$10–15 $M_{\odot}$, due to significant wind mass loss. Observations of BHs in X-ray binaries in the Galaxy are in accordance with a similar mass distribution (Farr et al. 2011).

Low-metallicity ($Z < 0.1\,Z_{\odot}$; $Z_{\odot}$ is the solar metallicity) star progenitors can remain more massive throughout their evolution as they undergo less wind mass loss and, therefore, they are likely to produce BHs of higher mass. It is generally believed that these low-metallicity stars are formed in the early universe (Dominik et al. 2015; Belczynski et al. 2016b), which seems to contradict the low redshift of the detected GW events (three with $z \sim 0.1$ and one with $z \sim 0.2$). However, by taking into consideration two factors, a long delay time from the birth of the BH binary to coalescence of $t_{\rm merge} \sim 10$ Gyr (Kinugawa et al. 2014), and a significantly higher low-metallicity star formation rate at low redshifts than previously thought (Hirschauer et al. 2016), this apparent conundrum is solved (Belczynski et al. 2016a).

Here, we propose an alternative evolutionary channel in which BHs with masses greater than $20\,M_{\odot}$ can form without the requirement of a low-metallicity environment. Specifically, a pair of stellar mass BHs are trapped by, and accrete mass from, an ambient accretion disk surrounding a supermassive black hole (SMBH) in an active galactic nucleus (AGN). There are a number of recent theoretical works studying related scenarios. In particular, models involving the formation, migration, trapping, hardening, and driven merger of SMBH binaries in an accretion disk of an SMBH have been studied most recently by McKernan et al. (2012), Stone et al. (2017), Bartos et al. (2017), and Leigh et al. (2018). However, based on a simple description of the binary interaction with the disk, it was found that little mass was accreted onto the BHs during their inspiral and migration. Here, we consider the same process, but based on the results of the most recent numerical study of the binary interaction with the circumbinary disk by Tang et al. (2017). It is found that there are possible circumstances under which BHs can accrete a non-negligible amount of material from the disk. In this case, there is no requirement for a low metallicity of the stellar population for the formation of high-mass stellar BHs ($>20\,M_{\odot}$).

In this Letter, we describe the evolution of binary BHs in terms of a model of mass accretion and orbital shrinkage of a system embedded in a circumbinary accretion disk in Section 2. With assumed distributions of the initial parameters of the binaries, the distribution of BH mass at coalescence is determined in Section 3, and the migration of the binary is discussed in Section 4. Finally, we summarize and discuss the implications of our results in the last section.

2. Accretion onto the Binary

For simplicity, we limit our discussion to the case of an equal mass binary ($M_1 = M_2 = m_{\rm BH}\,M_{\odot}$). This simplification can be justified by the results of Farris et al. (2014), who found that the mass ratio of a binary embedded within a disk tends to unity in a Keplerian circular orbit. Taking the time derivative of the expression of the orbital angular momentum, J, and with the further assumption that each BH in the binary is accreting at

the same rate, we obtain the following relation:

$$\frac{\dot{J}}{J} = \frac{3\dot{M}_{\rm bin}}{2M_{\rm bin}} + \frac{\dot{a}_J}{2a}, \quad (1)$$

where $M_{\rm bin} = 2\, m_{\rm BH}\, M_\odot$ and $m_{\rm BH}$ is the dimensionless mass of an individual BH, a is the orbital separation of the binary, and $\dot{a}_J$ is the time rate of change of a due to the exchange of angular momentum. The numerical simulations of Tang et al. (2017), which also take into account the dominant torques exerted on the binary system associated with the distortion of the mini disks surrounding the two BHs, can be described by the following empirical relation (with physical unit restored):

$$\dot{J} = (-0.21\ \tau_{\rm sink} + 0.437)\dot{M}_{\rm bin}\sqrt{GMa}\,, \quad (2)$$

where $\tau_{\rm sink}$ is the dimensionless sink timescale that describes the mass removal rate (due to accretion onto the BHs). We treat the net accretion rate onto individual BHs $\dot{m}_{\rm BH}$ and $\tau_{\rm sink}$ as independent parameters. This follows from the fact that $\tau_{\rm sink}$ alone does not determine the mass flow rate from the mini disk to the BH without providing the surface density of the mini disk. In addition, the net accretion rate can differ from the mass flow rate in the mini disk as result of, for example, outflows.

Combining Equations (1) and (2), we have

$$\frac{\dot{a}_J}{\dot{m}_{\rm BH}} = -\gamma\frac{a}{m_{\rm BH}}, \quad (3)$$

where $\gamma = 1.68\,\tau_{\rm sink} - 0.496$. Tang et al. (2017) mentioned that in any physical case $\tau_{\rm sink}$ should be larger than 2.1, and $\tau_{\rm sink} = 5$ corresponds to a slow sink.

The orbital shrinkage rate due to gravitational radiation is given by

$$\dot{a}_{12,\rm GW} = -7.88 \times 10^{-14} a_{12}^{-3} m_{\rm BH}^3, \quad (4)$$

where $\dot{a}_{12,\rm GW}$ is the $\dot{a}$ due to GW radiation in unit of 10^{12} cm yr^{-1}.

For accretion onto the BH, we assume that its rate is proportional to its mass,

$$\dot{m}_{\rm BH} = \eta m_{\rm BH}/\tau_{\rm acc}, \quad (5)$$

where $\tau_{\rm acc}$ is the Eddington accretion timescale equal to 10^8 years (assuming a radiative efficiency of $\sim$20%),[4] and η is the Eddington ratio.

The total change in the rate of the separation is given by $\dot{a} = \dot{a}_{\rm GW} + \dot{a}_J$, where it is assumed that the individual torque contributions can be linearly added. Although this is a common assumption, nonlinearities may result from distortions of the disk. Combining Equations (3), (5), and (6), and eliminating t, we obtain a differential equation between a and $m_{\rm BH}$:

$$\frac{da_{12}}{dm_{\rm BH}} = -\gamma\frac{a}{m_{\rm BH}} - 7.88 \times 10^{-6} a_{12}^{-3} m_{\rm BH}^2 \eta^{-1}. \quad (6)$$

The solution of Equation (6) is illustrated in Figure 1 for η ranging from 1 to 1000 and $\tau_{\rm sink}$ ranging from 3 to 5. Initially, for large a and small $M_{\rm BH}$, the shrinkage of a is dominated by the angular momentum transfer between the binary and the circumbinary disk. Therefore, the dependence of a on $M_{\rm BH}$ is

[4] A different choice of the radiative efficiency is equivalent to a variation in η.

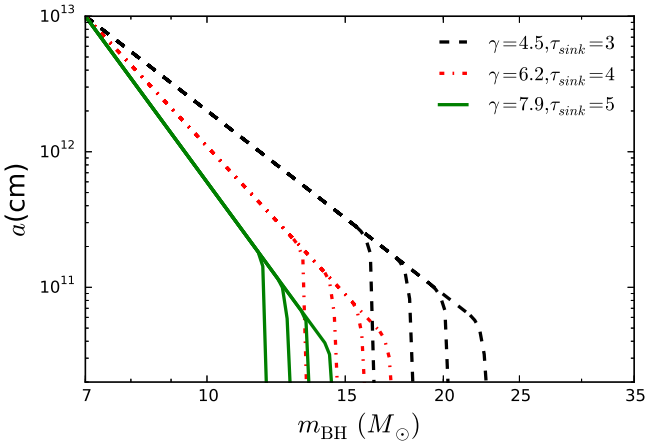

Figure 1. Shrinkage of the binary orbital separation as a function of the BH mass. Curves delineated with different line styles and colors correspond to $\tau_{\rm sink}$ from 3 to 5 (γ = 4.5–7.9). For each value of γ, four branches are shown corresponding to η = 1, 10, 100, and 1000, from left to right.

given by a power law

$$a = a_0\left(\frac{m_{\rm BH}}{m_{\rm BH,0}}\right)^{-\gamma}, \quad (7)$$

where a_0 and $m_{\rm BH,0}$ is the initial separation and the BH mass (dimensionless) respectively. When a is sufficiently small, GW radiation dominates the evolution, resulting in the turnover in Figure 1.

The final mass of the BH before coalescence can be evaluated approximately by equating the $\dot{a}_J$ and $\dot{a}_{\rm GW}$:

$$\gamma\frac{a_{12}}{m_{\rm BH}} = 7.88 \times 10^{-6} a_{12}^{-3} m_{\rm BH}^2 \eta^{-1}. \quad (8)$$

Eliminating a with Equation (7), we have

$$m_{\rm BH,c} = \left(\frac{a_{12,0}^4 \eta\gamma m_0^{4\gamma}}{7.88 \times 10^{-6}}\right)^{1/(3+4\gamma)}, \quad (9)$$

where $m_{\rm BH,c}$ and m_0 are the mass of the individual BH at GW-dominated coalescence and the initial mass of the BH, both in units of $M_\odot$; $a_{12,0}$ is the initial separation in units of 10^{12} cm. The mass evaluated with Equation (9) is conservative, because the binary can continue accreting until its merger. However, the correction to $m_{\rm BH,c}$ will be very small, considering the short duration of the plunging phase. Figure 1 clearly shows how a_0, $m_{\rm BH,0}$, $\tau_{\rm sink}$, and η determine the final mass $m_{\rm BH,c}$: a_0 is the intercept on the vertical axis when the BH has a mass of $m_{\rm BH,0}$; a larger value of $\tau_{\rm sink}$ yields a greater power-law slope on the declining portion, thus resulting in a smaller $m_{\rm BH,c}$; a larger value of η yields a larger $m_{\rm BH,c}$. It is found that the final mass $m_{\rm BH,c}$ is more sensitive to $\tau_{\rm sink}$ than to η.

3. Distribution of BH Mass at Coalescence

To determine the population distribution of $m_{\rm BH,c}$, the distribution of each parameter on the right side of Equation (9) is required. For definiteness, a Gaussian distribution of the initial mass of BHs is assumed, with the mean mass of $m_{{\rm BH},\mu} = 7.8(M_\odot)$ and the standard deviation $m_{{\rm BH},\sigma} = 1.2(M_\odot)$ (Özel et al. 2010; Farr et al. 2011). The parameter, γ, is calculated from $\tau_{\rm sink}$, the distribution of which is assumed to be

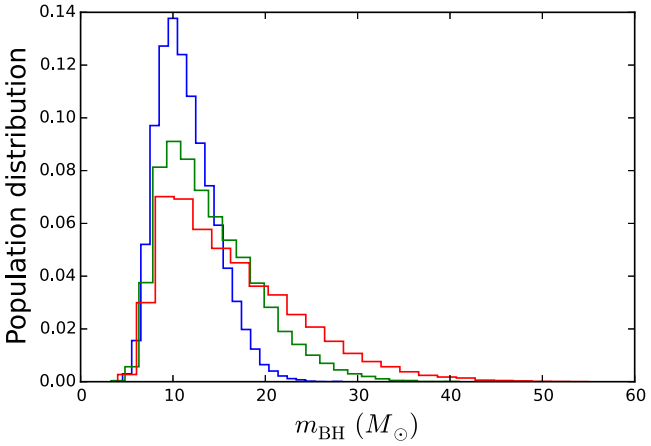

Figure 2. Population distribution of $m_{\rm BH,c}$. The blue histogram corresponds to the large a cutoff at 10^{13} cm, the green histogram corresponds to the large a cutoff at 10^{14} cm, and the red histogram corresponds to the cutoff at 6×10^{14} cm.

uniform from $\tau_{\rm sink}=3$ to $\tau_{\rm sink}=5$. Finally, the Eddington ratio, η, is assumed to range from 1 to 1000 log-uniformly.

The actual distribution of the orbital separation, a, of the binary BH system is uncertain. However, the Roche radius of the binary BH in orbit about the SMBH should provide an upper limit for a, for otherwise any binary would be torn apart by the tidal force of the SMBH. The Roche radius $R_{\rm R}$ is approximated by

$$a_{0,\rm max}=R_{\rm R}=\left(\frac{2m_{\rm BH}}{m_{\rm SMBH}}\right)^{1/3}R_0, \tag{10}$$

where R_0 is the initial distance from the binary to the SMBH. If we take the mass of the supermassive BH (in unit of $M_\odot$) $m_{\rm SMBH}\sim10^6$, $2\,m_{\rm BH}\sim10$, $R_0\sim0.01$ pc, then $R_{\rm R}\sim6\times10^{14}$ cm. Stellar interactions with the binary BH can affect the orbital separation distribution, and Bartos et al. (2017) considered the ionization of the binary by softening encounters with stars. In this context, the timescale of the ionization can be estimated by

$$t_{\rm ion}\approx10\times\frac{M_{\rm SMBH}}{M_{\rm bin}}t_{\rm orb}, \tag{11}$$

where $M_{\rm SMBH}$ is the mass of the SMBH and $t_{\rm orb}$ is the orbital period of the binary around the SMBH. For $M_{\rm SMBH}>10^6\,M_\odot$, $M_{\rm bin}=20\,M_\odot$ and $R=0.01$ pc, $t_{\rm ion}>5\times10^7$ years, which is orders of magnitude greater than the merger timescale. Therefore, we can safely ignore this process.

A flat distribution of a in log space is used, i.e., Öpik's law (Shatsky & Tokovinin 2002; Kobulnicky & Fryer 2007; Lépine & Bongiorno 2007) with a large a cutoff as the distribution of a. There should also be a cutoff at the small a, where the GW radiation dominates at the outset. This value can be found by setting $m_{\rm BH,c}=m_0$ in Equation (9):

$$a_{12,0,\rm min}=(7.88\times10^{-6}\eta^{-1}\gamma^{-1}m_0^3)^{1/4}. \tag{12}$$

The resulting population distribution of $M_{\rm BH,c}$ for a range of a cutoff values is plotted in Figure 2. The distribution of BH mass peaks at $\sim10\,M_\odot$, which is independent of the large a cutoff, although a larger cutoff extends the tail of the distribution to higher masses. In both distributions, there is a significant fraction of BHs that can increase their mass to greater than $20\,M_\odot$.

4. Migration to SMBH

Because the binary is trapped in the accretion disk of an AGN, it will migrate closer to the SMBH due to its interaction. If the orbital separation of the double BH binary system is much less than the scale height of the disk, the binary can be approximated by a massive point object. We use the disk-satellite interaction to estimate the timescale of migration. Specifically, Baruteau et al. (2011) have shown that if the object is sufficiently massive to open a gap in the disk, the horseshoe drag is much reduced and the Lindblad torque balances the viscous torque exerted by the disk (type II migration). The gap-opening criterion (Baruteau et al. 2011) is

$$\frac{3H}{4R_0}(q/3)^{-1/3}+50\alpha\left(\frac{H}{R_0}\right)^2/q<1. \tag{13}$$

For an SMBH with $\sim10^6\,M_\odot$, a binary BH with mass larger than $20\,M_\odot$ (with $\alpha=0.01$) meets the criterion of type II migration. In this case, the migration timescale is estimated using Equation (6) of Baruteau et al. (2011). We adopt $m_{\rm SMBH}=10^6$, and use the standard gas-pressure-dominated disk model (Shakura & Sunyaev 1973) $H/R_0\approx3\times10^{-3}$ with Kramer's opacity, $\alpha=0.01$, and $r_0=0.01$ pc. This yields $\tau_{\rm M}\approx1.1\times10^8$ years. Hence, for an Eddington ratio $\eta>\alpha/10^{-2}$, the migration timescale does not limit the growth of the BH mass via accretion for low-mass AGNs. For an AGN with $m_{\rm SMBH}>10^8$, the migration will be type I and the migration time is $\sim10^6$ years (Baruteau et al. 2011), which is too short for a significant mass increase of the binary.

5. Conclusion and Discussion

The nuclei of galaxies are known to be regions of high stellar density. The star formation rates can be high and the migration of massive objects toward the central region can be effective. Hence, it is possible that a large population of SMBHs could be harbored in this region, and some of them might be trapped in the gaseous disk around the AGN (Bartos et al. 2017). We show in this Letter that, given a super-Eddington accretion rate (η in range between $\sim$10 and 1000), SMBH binaries can accrete a significant amount of mass from a circumbinary disk before the GW radiation dominates the coalescence phase with a non-negligible fraction growing to $>20\,M_\odot$. The above mentioned evolutionary channel serves as an alternative pathway to produce the unusually massive SMBH binaries detected by LIGO.

5.1. The Validity of the Circular Orbit

The binary orbit in a hierarchical triplet may evolve into a large eccentricity due to the Kozai–Lidov mechanism (Kozai 1962; Lidov 1962). The first nonzero term of the Kozai–Lidov mechanism is the quadrupole term, which vanishes when the inclination of the inner orbit is smaller than a critical value of $\sim39.^\circ2$. In the next order, i.e., the octupole Kozai–Lidov mechanism, a nearly coplanar inner orbit with very small initial eccentricity will not evolve into a large eccentricity (Lee & Peale 2003; Li et al. 2014). Therefore, we limit our discussion

to an initially coplanar and circular orbit, which is stable and self-consistent.

5.2. Accretion Rate onto the Binary

Here, we examine the consistency for a super-Eddington accretion rate corresponding to $\eta = 1$–1000, given the densities in the AGN disk. An upper limit of the accretion rate onto the binary can be estimated (as in Equation (2) of Stone et al. 2017) with

$$\dot{M} = \pi \rho \sigma_{\rm gas} r_{\rm acc} \min[r_{\rm acc}, H], \tag{14}$$

where ρ and H are the density and scale height of the AGN disk, respectively, and $r_{\rm acc}$ is the radius of accretion

$$r_{\rm acc} = \frac{GM_{\rm bin}}{\sigma_{\rm gas}^2}, \tag{15}$$

where σ^2 is the squared sum of three terms: (1) the sound speed of the gas c_s, (2) the velocity shear across the Hill radius of the binary, and (3) the relative velocity between the binary and the disk due to eccentric and inclined orbit (see Stone et al. 2017). In this Letter, we consider the binaries in a coplanar and circular orbit around the SMBH and, therefore, the third term in $\sigma_{\rm gas}^2$ vanishes. ρ can be estimated with the formula of a standard thin disk:

$$\rho = 5 \times 10^{-11} \left(\frac{\alpha}{0.01}\right)^{-7/10} \eta_{\rm SMBH}^{11/20} \left(\frac{M_{\rm SMBH}}{10^6\, M_\odot}\right)^{47/40} \times \left(\frac{R_0}{0.01\ {\rm pc}}\right)^{-15/8} {\rm g\ cm^{-3}}, \tag{16}$$

where $\eta_{\rm SMBH}$ is the Eddington ratio of the SMBH. For $M_{\rm SMBH} \sim 10^6\, M_\odot$, $R_0 = 0.01$ pc, $\alpha = 0.01$, and $M_{\rm bin} = 20\, M_\odot$, we find that $\dot{M}$ is larger than 10^3 times of the Eddington rate of the binary as long as $\eta_{\rm SMBH} > 0.01$. When the orbit of the binary is retrograde with respect to the accretion disk of the AGN, the relative velocity between the binary and the gas in the accretion disk dominates $\sigma_{\rm gas}^2$. As a result, the mass inflow rate is much smaller and insufficient to support the required accretion rate. Therefore, we limit our discussion in this Letter to the case of a prograde orbit. In the case of super-Eddington accretion, the actual accretion rate onto the BH could be only a fraction of the total matter inflow rate, because substantial mass loss in an outflow is expected (see recent works of Yang et al. 2014 and Jiang et al. 2014). Hence, the accretion rate in this Letter refers to the net value onto the individual BH. $R_0 = 0.01$ pc is taken as a reference value in the above discussion. For larger radii ($R_0 > 0.1$ pc), the AGN disk is no longer stable under its self-gravity and, thus, star formation becomes important (Stone et al. 2017). As a consequence, the physical picture might need modification.

5.3. Observational Consequences

In our channel, SMBHs can accrete several times their initial mass from the accretion disk. We thus expect that the resulting BHs can become extreme Kerr BHs before coalescence with their spin axes aligned. For such systems, the results of numerical simulations (Healy et al. 2014) indicate that the total energy loss in GW radiation would be ~10% of the rest mass energy, or 2–3 times higher than in the case for a random orientation. Although the currently detected GW events do not provide support for such progenitors, future events may be found that correspond to rapidly spinning and aligned BHs, a likely consequence of our model.

A natural expectation in this formation channel of such GW sources is that they are associated with AGNs. The super-Eddington accretion onto the BH binary (BHB) can give rise to luminous X-ray emission, which may outshine a sub-Eddington accreting AGN in the same wavelength band (see Bartos et al. 2017 and Stone et al. 2017). Furthermore, after the coalescence of the BHB, remnant matter from the mini disk may fall back onto the newly formed Kerr BH at an even higher rate. Such a possibility may trigger the formation of a relativistic jet through the Blandford–Znajek mechanism (Blandford & Znajek 1977). As pointed out by Bartos et al. (2017), a gamma-ray burst-like counterpart could be produced in this case. In addition to the radiation at high energies, the jet might also give rise to coherent radio emission, which will be the topic of a future paper.

The authors appreciate the suggestions from anonymous reviewers that greatly improved the manuscript. K.S.C. and S.X.Y. are supported by a GRF grant under 17310916.

ORCID iDs

Shu-Xu Yi https://orcid.org/0000-0001-7599-0174
K. S. Cheng https://orcid.org/0000-0002-8043-9851
Ronald E. Taam https://orcid.org/0000-0001-8805-2865

References

Abbott, B. P., Abbott, R., Abbott, T. D., et al. 2016a, PhRvX, 6, 041015
Abbott, B. P., Abbott, R., Abbott, T. D., et al. 2016b, PhRvL, 116, 241103
Abbott, B. P., Abbott, R., Abbott, T. D., et al. 2017a, PhRvL, 118, 221101
Abbott, B. P., Abbott, R., Abbott, T. D., et al. 2017b, PhRvL, 119, 141101
Bartos, I., Kocsis, B., Haiman, Z., & Márka, S. 2017, ApJ, 835, 165
Baruteau, C., Cuadra, J., & Lin, D. N. C. 2011, ApJ, 726, 28
Belczynski, K., Holz, D. E., Bulik, T., & O'Shaughnessy, R. 2016a, Natur, 534, 512
Belczynski, K., Repetto, S., Holz, D. E., et al. 2016b, ApJ, 819, 108
Blandford, R. D., & Königl, A. 1979, ApJ, 232, 34
Blandford, R. D., & Znajek, R. L. 1977, MNRAS, 179, 433
Dominik, M., Berti, E., O'Shaughnessy, R., et al. 2015, ApJ, 806, 263
Farr, W. M., Sravan, N., Cantrell, A., et al. 2011, ApJ, 741, 103
Farris, B. D., Duffell, P., MacFadyen, A. I., & Haiman, Z. 2014, ApJ, 783, 134
Fryer, C. L., & Kalogera, V. 2001, ApJ, 554, 548
Healy, J., Lousto, C. O., & Zlochower, Y. 2014, PhRvD, 90, 104004
Hirschauer, A. S., Salzer, J. J., Skillman, E. D., et al. 2016, ApJ, 822, 108
Jiang, Y.-F., Stone, J. M., & Davis, S. W. 2014, ApJ, 796, 106
Kinugawa, T., Inayoshi, K., Hotokezaka, K., Nakauchi, D., & Nakamura, T. 2014, MNRAS, 442, 2963
Kobulnicky, H. A., & Fryer, C. L. 2007, ApJ, 670, 747
Kozai, Y. 1962, AJ, 67, 591
Lee, M. H., & Peale, S. J. 2003, ApJ, 592, 1201
Leigh, N. W. C., Geller, A. M., McKernan, B., et al. 2018, MNRAS, 474, 5672
Lépine, S., & Bongiorno, B. 2007, AJ, 133, 889
Li, G., Naoz, S., Kocsis, B., & Loeb, A. 2014, ApJ, 785, 116
Lidov, M. L. 1962, P&SS, 9, 719
McKernan, B., Ford, K. E. S., Lyra, W., & Perets, H. B. 2012, MNRAS, 425, 460
Özel, F., Psaltis, D., Narayan, R., & McClintock, J. E. 2010, ApJ, 725, 1918
Shakura, N. I., & Sunyaev, R. A. 1973, A&A, 24, 337
Shatsky, N., & Tokovinin, A. 2002, A&A, 382, 92
Stone, N. C., Metzger, B. D., & Haiman, Z. 2017, MNRAS, 464, 946
Tang, Y., MacFadyen, A., & Haiman, Z. 2017, MNRAS, 469, 4258
Yang, X.-H., Yuan, F., Ohsuga, K., & Bu, D.-F. 2014, ApJ, 780, 79